Available online at www.sciencedirect.com
SCIENCE DIRECT®
Journal of Solid State Chemistry 170 (2003) 182–187
JOURNAL OF SOLID STATE CHEMISTRY
http://elsevier.com/locate/jssc

Preparation and crystal structure analysis of CeCuOS

Kazushige Ueda,* Kouhei Takafuji, and Hideo Hosono

Materials and Structures Laboratory, Tokyo Institute of Technology, 4259, Natatsuta, Midori, Yokohama 226-8503, Japan

Received 30 May 2002; received in revised form 5 September 2002; accepted 25 September 2002

Abstract

A single phase of CeCuOS was prepared by sulfurization of starting materials, $CeO_2 + Cu_2S$, and subsequent post-annealing in evacuated silica tubes. The crystal structure of the CeCuOS single phase was examined by the Rietveld analysis. The shrinkage of the unit-cell volume for CeCuOS was obviously observed in the series of *Ln*CuOS (*Ln* = La–Nd) oxysulfides. The examination of interatomic distances revealed that Ce–S distances in CeCuOS are shorter than those predicted from the lanthanide contraction and this short Ce–S bond length is responsible for the unit-cell-volume shrinkage of CeCuOS. The origin of the shrinkage is discussed in the viewpoints of the Ce valence and interatomic distances along with the results of magnetic measurements.

Keywords: CeCuOS; Layered oxysulfide; Rietveld analysis; Magnetic moments bond valence

1. Introduction

Lanthanide copper oxychalcogenides, *Ln*CuO*Ch* (*Ln* = lanthanide, *Ch* = chalcogen) belong to mixed-anion materials composed of divalent oxygen and chalcogen anions. Although each cation in oxychalcogenides is usually coordinated by both oxygen and chalcogen anions, the situation in the *Ln*CuO*Ch* oxychalcogenides differs because of their layered crystal structure: Cu ions are coordinated by only chalcogen anions [1–5]. The crystal structure of *Ln*CuO*Ch* is shown in Fig. 1. The $(Ln_2O_2)^{2+}$ oxide layers and $(Cu_2Ch_2)^{2-}$ chalcogenide layers are alternately stacked along the *c*-axis, and the structure of each layer is regarded as a PbO-type and anti-PbO-type, respectively. This layered crystal structure brings interesting electrical and optical properties to these materials [6–12].

Charkin et al. first prepared CeCuOS along with other *Ln*CuOS (*Ln* = Sm, Eu) oxysulfides [13,14]. They reported the lattice constants of the series of *Ln*CuOS (*Ln* = La–Eu), and found anomalous shrinkage of the unit-cell volume for CeCuOS in the plot of the unit-cell volume against the atomic number of the lanthanide elements. However, some CeCuOS samples prepared by their group were not of a single phase but mixture of CeCuOS and Cu metal or Ce sulfide, and the details of the crystal structure of this material were not investigated.

In this study, we prepared a single phase of CeCuOS by a two-step process of sulfurization and post-annealing, and examined the crystal structure of this material by the Rietveld analysis. The dependence of the unit-cell volume on the lanthanide ions in the *Ln*CuOS (*Ln* = La–Nd) oxysulfides was reexamined to discuss the origin of the anomalous shrinkage for CeCuOS in the viewpoints of the valence states of Ce ions and interatomic distances.

2. Experiments

2.1. Sample preparation

*Ln*CuOS oxysulfides are usually synthesized by solid-state reaction of Ln_2O_3, Ln_2S_3 and Cu_2S, or Ln_2O_2S and Cu_2S in evacuated silica tubes. Although lanthanide metals can be used as starting materials, these lanthanide compounds are frequently used to avoid the oxidation of the metals. However, in the case of CeCuOS, Ce_2O_3 is not used as a starting material because Ce_2O_3 is unstable and oxidized to CeO_2.

*Corresponding author. Fax: 45-924-5339.
E-mail address: kueda@msl.titech.ac.jp (K. Ueda).

0022-4596/03/$ - see front matter © 2002 Elsevier Science (USA). All rights reserved.
PII: S0022-4596(02)00061-0

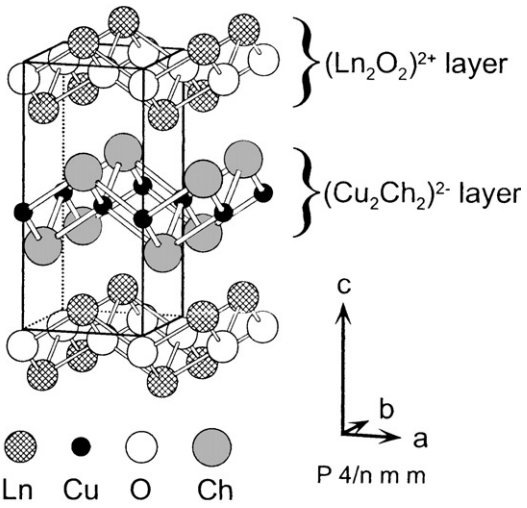

Fig. 1. Crystal structure of *Ln*CuO*Ch* (*Ln* = lanthanide, *Ch* = chalcogen).

Moreover, Ce_2O_2S is also unstable in air and easily oxidized by incorporating oxygen ions in its layered structure accompanying the change of the lattice constants and the color of the material [15]. Therefore, the use of Ce metal seems to be inevitable for the synthesis of CeCuOS by solid-state reaction in evacuated silica tubes. However, as Charkin et al. reported, the synthesis of a CeCuOS single phase seems to be very difficult probably because of the redox reaction of Ce and Cu ions. We also attempted this method but failed in obtaining a single-phase material.

We prepared CeCuOS through a two-step process, sulfurization and post-annealing. The sulfurization was carried out using H_2S gas, and post-annealing was done in evacuated silica tubes. Mixed powders of CeO_2 and Cu_2S (CeO_2:Cu_2S = 2:1) were used as starting materials, and the powder was sulfurized at 800°C for 2 h in the flow of the dilute H_2S gas composed of H_2S:H_2:Ar = 3:27:20. This reaction is expressed by the following equation:

$$2CeO_2 + Cu_2S + 2H_2S \rightarrow 2CeCuOS + 2H_2O + S.$$

However, the product of this reaction is not a single phase in the as-prepared state and includes a slight amount of other phases such as sulfide or oxide. The product was subsequently annealed at 800°C for 6 h in an evacuated silica tube to obtain a single phase of CeCuOS.

*Ln*CuOS (*Ln* = La, Pr, Nd) oxysulfides were synthesized by conventional solid-state reaction of Ln_2O_2S and Cu_2S in evacuated silica tubes to compare structural differences among the *Ln*CuOS (La–Nd) oxysulfides.

2.2. Characterization

The chemical composition of the sample was examined by inductively coupled plasma (ICP) emission spectroscopy. A small amount of the sample powder was dissolved in hot nitric acid at 130°C using an autoclave, and the solution was used for the ICP measurement.

The powder X-ray diffraction (XRD) pattern of the sample was recorded at room temperature using an XRD diffractometer with a rotary Cu target and a monochrometer for $K\alpha_1/K\alpha_2$ separation (Rigaku Rint, 2000). The intensity data collected from $2\theta = 5^\circ$ to 100° with a scan step of 0.02° were analyzed by the Rietveld method using the program code, RIETAN [16]. The space group of $P4/nmm$ was adopted for CeCuOS, and the crystal structural data reported for LaCuOS [1] were used as initial parameters in the calculation. The crystal structures of *Ln*CuOS (*Ln* = La, Pr, Nd) oxysulfides were also examined by the Rietveld analysis in the similar way.

Electrical conductivities were measured by the four-probe method using sintered disks. DC magnetic susceptibilities were measured with a SQUID magnetometer (Quantum Design, Model MPMS) in the temperature range from 5 to 273 K.

3. Results and discussion

The XRD pattern observed for the sample and the fitted pattern by the Rietveld analysis are shown in Fig. 2. The fitted pattern agrees well with the observed XRD pattern, confirming that the sample consists of a single phase of CeCuOS. The chemical composition of the sample analyzed by the ICP measurement revealed that the cation ratio of Cu/Ce is 0.99 ± 0.01. The single phase of CeCuOS shows black color and relatively high electrical conductivity ($\sigma = 1\,S\,cm^{-1}$) at room temperature. These features are unique for this material among *Ln*CuOS: the *Ln*CuOS (*Ln* = La, Pr, Nd) oxysulfides show light brown color and low electrical conductivities ($\sigma < 10^{-3}\,S\,cm^{-1}$) at room temperature.

The lattice constants, *a* and *c*, refined by the Rietveld analysis are summarized in Table 1 along with the unit-cell volume and *R* values. Table 2 lists atomic positions, isotropic thermal parameters (*B*), and site-occupancy parameters (*g*). Nominal chemical composition was assumed for the site-occupancy parameters in the Rietveld calculation because the Cu/Cu ratio examined by the ICP measurement was almost of stoichiometry. Although the possibility of Cu deficiency cannot be eliminated due to the Cu/Cu ratio and the large thermal parameter, the amount of Cu vacancies is considered to be rather small.

Lauxmann et al. synthesized single crystals of PrCuOS and analyzed its crystal structure [5]. Ishikawa et al. prepared some *Ln*CuOS (*Ln* = La, Pr, Nd) oxysulfides and examined the thermoelectric power of these materials [9]. However, they did not attempt to

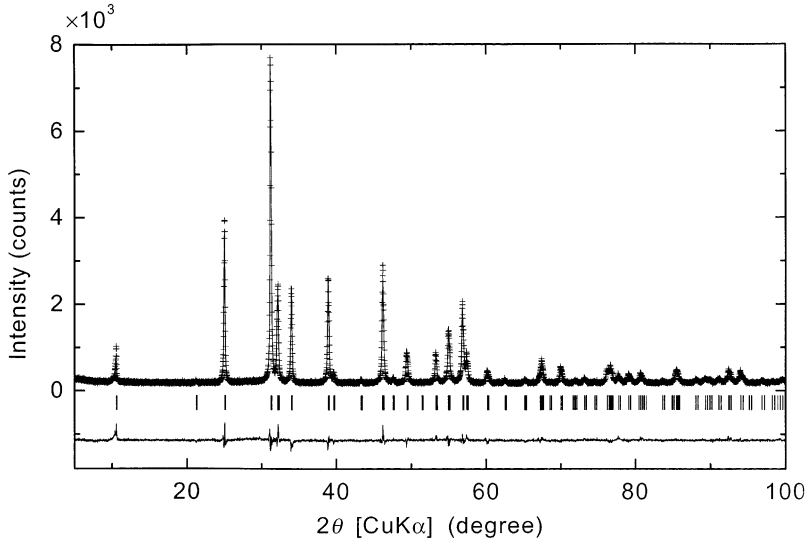

Fig. 2. XRD pattern of CeCuOS. Observed pattern (+) and calculated pattern (solid line) are shown along with their difference. The vertical bars indicate the position of Bragg reflections.

Table 1
Summary of refinement data and lattice parameters for *Ln*CuOS (*Ln* = La–Nd)

Formula	LaCuOS	CeCuOS	PrCuOS	NdCuOS
Space group	*P*4/*nmm*	*P*4/*nmm*	*P*4/*nmm*	*P*4/*nmm*
a (Å)	3.99625(4)	3.9228(1)	3.94148(9)	3.9196(1)
c (Å)	8.51743(9)	8.3475(3)	8.4376(1)	8.4282(2)
V_{cell} (Å^3)	136.023(2)	128.46(1)	131.081(5)	129.487(6)
Z	2	2	2	2
R_p	3.91	6.27	6.69	6.61
R_{wp}	5.34	8.21	8.50	8.55
R_e	3.38	5.80	5.96	4.66
S	1.57	1.41	1.42	1.83

Table 2
Site occupancy, atomic positions and istropic thermal parameters for *Ln*CuOS (*Ln* = La–Nd)

	WN	*g*	*x*	*y*	*z*	*B* (Å^2)
LaCuOS						
La	2*c*	1.00	1/4	1/4	0.1478(3)	0.4(1)
Cu	2*b*	1.00	1/4	3/4	1/2	1.7(2)
S	2*c*	1.00	1/4	1/4	0.661(1)	0.7(3)
O	2*a*	1.00	1/4	3/4	0	0.2(7)
CeCuOS						
Ce	2*c*	1.00	1/4	1/4	0.1508(6)	0.5(1)
Cu	2*b*	1.00	1/4	3/4	1/2	4.8(5)
S	2*c*	1.00	1/4	1/4	0.670(2)	0.2(4)
O	2*a*	1.00	1/4	3/4	0	0.2(4)
PrCuOS						
Pr	2*c*	1.00	1/4	1/4	0.1461(4)	0.2(1)
Cu	2*b*	1.00	1/4	3/4	1/2	1.2(3)
S	2*c*	1.00	1/4	1/4	0.663(1))	0.7(4)
O	2*a*	1.00	1/4	3/4	0	0.(1)
NdCuOS						
Nd	2*c*	1.00	1/4	1/4	0.1444(4)	0.4(2)
Cu	2*b*	1.00	1/4	3/4	1/2	1.2(3)
S	2*c*	1.00	1/4	1/4	0.666(1)	0.8(5)
O	2*a*	1.00	1/4	3/4	0	0.(1)

synthesize CeCuOS. Charkin et al. elaborately prepared several *Ln*CuO*Ch* (*Ch* = S, Se, Te) oxychalcogenides and found the anomalous shrinkage of the unit-cell volume for CeCuO*Ch*, which is not easily expected from the lanthanide contraction. However, some CeCuO*Ch* samples ($CeCu_{1.0}O$*Ch* and $CeCu_{0.8}O$*Ch*) that they prepared were the mixture of CeCuO*Ch* and Cu metal or Ce chalcogenide. Since the presence of the secondary phases might influence the lattice constants of the CeCuO*Ch* oxychalcogenides, we reexamined the dependence of the unit-cell volume on the lanthanide ions in the *Ln*CuOS (*Ln* = La–Nd) oxysulfides using single-phase samples. Figs. 3(a) and (b) show the unit-cell volume and lattice constants for *Ln*CuOS. Our results are similar to those reported by Charkin et al. and the unit-cell-volume shrinkage for CeCuOS was observed obviously. It is, therefore, concluded that the shrinkage for CeCuOS is intrinsic to this compound.

DC magnetic susceptibility (χ) was measured to evaluate effective magnetic moments (μ_{eff}) for *Ln*CuOS (La–Nd). LaCuOS showed diamagnetic behavior. While other oxysulfides showed paramagnetic behavior. The plot of $1/\chi - T$ demonstrated that the paramagnetic samples basically obey the Curie–Weiss law, and the effective magnetic moments were estimated to be $\mu_{eff} = 2.1\,\mu_B$ for CeCuOS, $3.1\,\mu_B$ for PrCuOS and $3.3\,\mu_B$ for NdCuOS (μ_B: Bohr magneton). These values are slightly different from those of free Lanthanide trivalent ions,

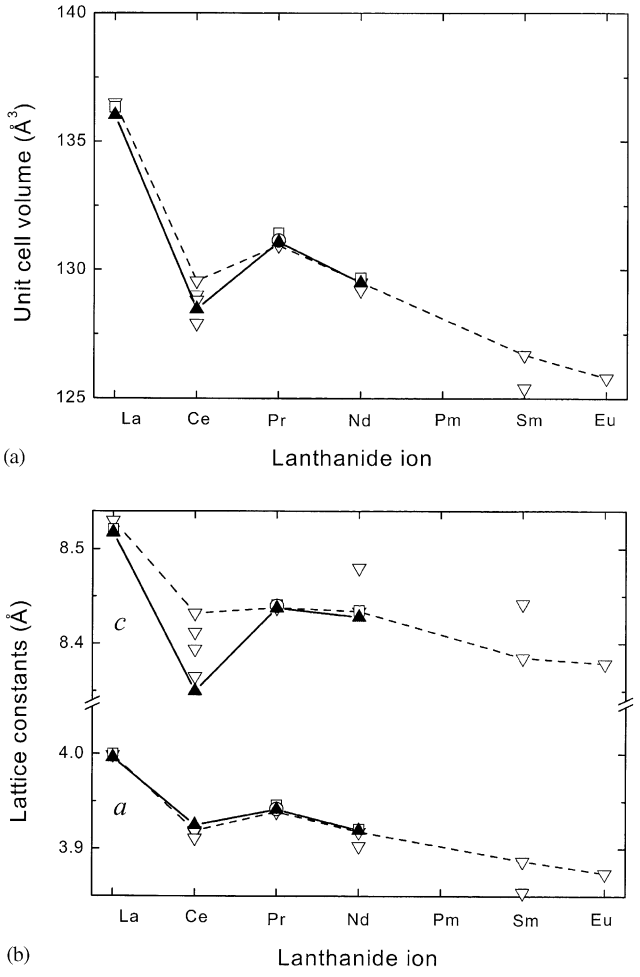

Fig. 3. Unit-cell volume (a) and lattice constants (b) of *Ln*CuOS against lanthanide ions. The data obtained in this study (filled triangle) are shown with the data reported by Charkin et al. (open triangle), Ishikawa et al. (open square), and Lauxmann et al. (open circle) for comparison.

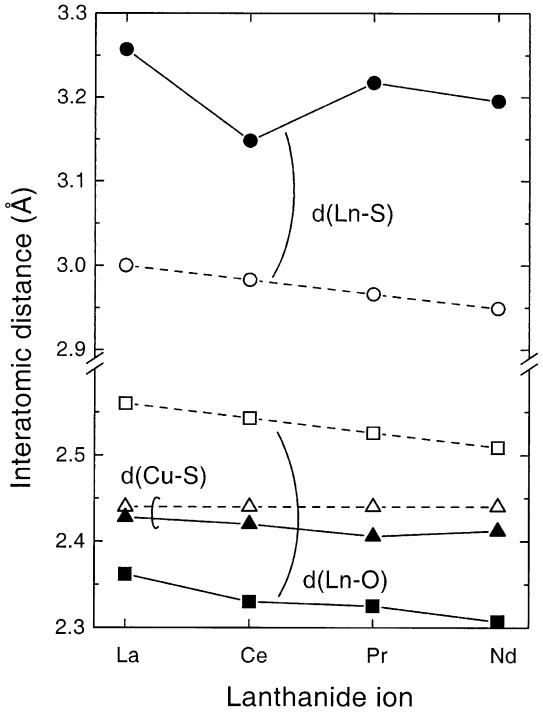

Fig. 4. Observed (closed symbol) and calculated (open symbol) interatomic distances in *Ln*CuOS against lanthanide ions. *Ln*–O (square), *Ln*–S (circle), and Cu–S (triangle).

Table 3
Observed and calculated interatomic distances in *Ln*CuOS

Sample	Ln–O (Å)		Ln–S (Å)		Cu–S (Å)	
	Obs.	Cal.	Obs.	Cal.	Obs.	Cal.
LaCuOS	2.362(1)	2.56	3.257(6)	3.00	2.428(7)	2.44
CeCuOS	2.330(2)	2.54	3.148(8)	2.98	2.42(1)	2.44
PrCuOS	2.325(2)	2.53	3.217(7)	2.97	2.406(8)	2.44
NdCuOS	2.307(2)	2.51	3.195(8)	2.95	2.412(9)	2.44

$\mu_{\mathrm{eff}} = 2.4\,\mu_{\mathrm{B}}$ for Ce^{3+}, $3.5\,\mu_{\mathrm{B}}$ for Pr^{3+} and $3.5\,\mu_{\mathrm{B}}$ for Nd^{3+}, probably due to the influence of the crystal field [17]. Similar results on the effective magnetic moments have been reported for *Ln*CuOSe (*Ln* = Ce, Nd) by Ohtani et al. [7]. The effective magnetic moment for CeCuOS indicates that Ce ions are primarily trivalent in this material.

To understand the unit-cell-volume shrinkage of CeCuOS, the interatomic distances in *Ln*CuOS were examined. The interatomic distances were estimated from the analyzed crystal data and plotted against the lanthanide ions as shown in Fig. 4. The interatomic distances are also calculated from the data of ionic radii [18] by summing the ionic radii of neighboring ions, and the observed and calculated data are listed in Table 3 and compared in Fig. 4. The ionic radii for eight-fold coordinated Ln^{3+} ions are used in the calculation of the interatomic distances. In comparison between the observed interatomic distances and the calculated ones, it is understood that the observed *Ln*–S distances are longer than the calculated ones, while the situation is reverse in the *Ln*–O distances. The observed Cu–S distances are very close to the calculated ones. This long *Ln*–S distances or short *Ln*–O distances in *Ln*CuOS indicate that the chemical bonds between *Ln* and S ions are weaker than those between *Ln* and O ions. As a consequence, the crystal structure of *Ln*CuOS can be regarded as a layered structure from a viewpoint of the interatomic distances as well as the atomic arrangements in the crystal [19].

Another important observation in Fig. 4 is that only the *Ln*–S distances do not obey the tendency anticipated from the lanthanide contraction: the Ce–S distance is obviously shorter than that predicted from the tendency. Therefore, it is concluded that this short

Ce–S distance is responsible for the shrinkage of the unit-cell volume for CeCuOS. The bond–valence calculation was carried out to estimate the valence of the lanthanide ions from the interatomic distances. Using the bond–valence parameters reported by Brown et al. [20] and Brese et al. [21], the valence of the lanthanide ions in *Ln*CuOS was calculated to be 3.15 for La ions, 3.43 for Ce ions, 3.17 for Pr ions and 3.10 for Nd ions. These valence states demonstrate that Ce ions in CeCuOS have higher valence than the other lanthanide ions. Although the effective magnetic moment of CeCuOS may not support the valence of the Ce ions as high as 3.43, this higher valence suggests that the Ce ions in CeCuOS have larger covalency with neighboring anions, especially S ions.

Charkin et al. [13] discussed this anomalous shrinkage of the unit-cell volume for CeCuOS in terms of the redox reaction between Ce and Cu ions: $Ce^{3+} + Cu^{+} \leftrightarrow Ce^{4+} + Cu^{0}$. They suggested that the presence of Ce^{4+} ($r_i = 0.97$ Å) and its similar ionic radius than Ce^{3+} ($r_i = 1.143$ Å) caused a decrease in the unit-cell volume. However, there is no clear evidence of the redox reaction or the presence of Ce^{4+} and/or Cu^{0} in the lattice so far. In the case of Ce oxysulfides including a Ce^{4+} valence state, the short Ce–O distances, d(Ce–O), are always observed in their crystals due to the small Ce^{4+} ionic radius: d(Ce–O) = 2.29 Å for $Ce_2O_{2.5}S$ [15] and 2.17 Å for $Ce_4O_4S_4$ [22] or $Ce_6O_6S_4$ [23]. As shown in Fig. 4, the Ce–O distances in CeCuOS almost follow a linear variation predicted from the lanthanide contraction, and no short Ce–O bonds were obviously found in the crystal structure. Instead of the absence of the short Ce–O bonds, this study demonstrated that the shrinkage of the unit-cell volume for CeCuOS originates from the short Ce–S bonds. According to these interatomic distances and the effective magnetic moment in CeCuOS, it is unlikely that a significant amount of Ce^{4+} ions is generated enough to cause the unit-cell-volume shrinkage due to the small ionic radius. Although the possibility of the presence of the Ce^{4+} ions is not thoroughly eliminated, it seems that the shrinkage would not be explained simply by the redox reaction between Ce and Cu ions and the small Ce^{4+} radius. The short Ce–S distances will be interpreted as a result of the increase of convalency in the Ce–S bonds. Since complex electronic states of Ce^{3+} ions have been observed frequently in some covalent Ce^{3+}-compounds [24], we suppose that a rather complicated hybridized state of Ce 4*f*, 5*d*, Cu 3*d*, 4*s* and S 3*p* orbitals is associated with the anomalous shrinkage in CeCuOS. This hybridized state will be suggested by the observation that only CeCuOS shows black color and high electrical conductivity among *Ln*CuOS. However, the origin of the short Ce–S bond length and the details of the electronic states of the Ce–S bonds is still open question in CeCuOS.

Further studies such as electronic structure analysis by photoemission spectroscopy are necessary to understand the unique features in CeCuOS.

4. Conclusion

A single phase of CeCuOS was prepared by a two-step process, and its crystal structure was examined by the Rietveld analysis. The lattice constants and unit-cell volume of CeCuOS estimated in this study are in reasonable agreement with those reported by Charkin et al. and the anomalous shrinkage of the unit-cell volume for this material was confirmed using the single-phase sample. The magnetic measurement demonstrated that the effective magnetic moment of CeCuOS is close to that of free Ce^{3+} ions, indicating that Ce ions are primarily trivalent in this material. The examination of interatomic distances revealed that the shrinkage is derived from the short Ce–S distances, and no short Ce–O bonds were found in this material. These results suggest that covalency or hybridization of orbitals is important in the Ce–S bonds, and the shrinkage of the unit-cell volume would not be attributed easily to the smaller ionic radius of tetravalent Ce ions generated by the simple redox reaction between Ce and Cu ions.

References

[1] M. Palazzi, Sci. Acad. Paris C. R. 292 (1981) 789.
[2] W.J. Zhu, Y.Z. Huang, C. Dong, Z.X. Zhao, Mater. Res. Bull. 29 (1994) 143.
[3] A.M. Kusainova, P.S. Berdonosov, L.G. Akselrud, L.N. Kholodkovskaya, V.A. Dolgikh, B.A. Popovkin, J. Solid State Chem. 112 (1994) 189.
[4] P.S. Berdonosov, A.M. Kusainova, L.N. Kholodkovskaya, V.A. Dolgikh, L.G. Akselrud, B.A. Popovkin, J. Solid State Chem. 118 (1995) 74.
[5] P. Lauxmann, T. Schleid, Z. Anorg. Allg. Chem. 626 (2000) 2253.
[6] Y. Takano, K. Yahagi, K. Sekizawa, Physica B 206 & 207 (1995) 764.
[7] T. Ohtani, M. Hirose, T. Sato, K. Nagaoka, M. Iwabe, Jpn. J. Appl. Phys. 32 (Suppl. 32-3) (1993) 316.
[8] T. Ohtani, Y. Tachibana, Y. Fujii, J. Alloys Compds. 262–263 (1997) 175.
[9] K. Ishikawa, S. Kinoshita, Y. Suzuki, S. Matsuura, T. Nakanishi, M. Aizawa, Y. Suzuki, J. Electrochem. Soc. 138 (1991) 1166.
[10] K. Ueda, S. Inoue, S. Hirose, H. Kawazoe, H. Hosono, Appl. Phys. Lett. 77 (2000) 2701.
[11] K. Ueda, S. Inoue, H. Hosono, N. Sarukura, H. Hirano, Appl. Phys. Lett. 78 (2001) 2333.
[12] K. Ueda, H. Hosono, J. Appl. Phys. 91 (2002) 2333.
[13] D.O. Charkin, A.V. Akopyan, V.A. Dolgikh, Russ. J. Inorg. Chem. 44 (1999) 833.

[14] B.A. Popvkin, A.W. Kusainova, V.A. Dolgikh, L.G. Aksel'rud, Russ. J. Inorg. Chem. 43 (1998) 1471.
[15] R. Mauricot, J. Gareh, M. Evain, Z. Kristallogr 212 (1997) 24.
[16] F. Izumi, in: R.A. Young (Ed.), The Rietveld Method, Oxford University Press, London, 1993.
[17] D.A. Maclean, K. Seto, J.E. Greedan, J. Solid State Chem. 40 (1981) 241.
[18] R.D. Shannon, Acta Crystallogr. A 32 (1976) 751.
[19] K. Ueda, H. Hosono, Thin Solid Films 411 (2002) 115.
[20] I.D. Brown, D. Altermatt, Acta Crystallogr. B 41 (1985) 244.
[21] N.E. Brese, M. O'Keefe, Acta Crystallogr. B 47 (1991) 192.
[22] J. Dugue, D. Carre, M. Guittard, Acta Crystallogr. B 34 (1978) 3564.
[23] J. Dugue, D. Carre, M. Guittard, Acta Crystallogr. B 35 (1979) 1550.
[24] A. Fujimori, J.H. Weaver, Phys. Rev. B 31 (1985) 6345.